Virology 413 (2011) 310–319

Contents lists available at ScienceDirect

Virology

journal homepage: www.elsevier.com/locate/yviro

A membrane-associated movement protein of *Pelargonium flower break virus* shows RNA-binding activity and contains a biologically relevant leucine zipper-like motif

Sandra Martínez-Turiño, Carmen Hernández *

Instituto de Biología Molecular y Celular de Plantas, Consejo Superior de Investigaciones Científicas-Universidad Politécnica de Valencia, Ciudad Politécnica de la Innovación, Ed. 8E. Camino de Vera s/n, 46022 Valencia, Spain

ARTICLE INFO

Article history:
Received 27 January 2011
Returned to author for revision
11 February 2011
Accepted 3 March 2011
Available online 27 March 2011

Keywords:
Carmovirus
PFBV
Movement proteins
RNA-binding domain
Leucine zipper-like motif
Membrane association
Subcellular localization

ABSTRACT

Two small viral proteins (DGBp1 and DGBp2) have been proposed to act in a concerted manner to aid intra- and intercellular trafficking of carmoviruses though the distribution of functions and mode of action of each protein partner are not yet clear. Here we have confirmed the requirement of the DGBps of *Pelargonium flower break virus* (PFBV), p7 and p12, for pathogen movement. Studies focused on p12 have shown that it associates to cellular membranes, which is in accordance to its hydrophobic profile and to that reported for several homologs. However, peculiarities that distinguish p12 from other DGBps2 have been found. Firstly, it contains a leucine zipper-like motif which is essential for virus infectivity in plants. Secondly, it has an unusually long and basic N-terminal region that confers RNA binding activity. The results suggest that PFBV p12 may differ mechanistically from related proteins and possible roles of PFBV DGBps are discussed.

Introduction

To establish a productive infection, plant viruses need to move from their replication sites to and through plasmodesmata (PD), which are wall spanning co-axial membranous organelles that bridge the cytoplasm of contiguous cells (Benitez-Alfonso et al., 2010). Such intracellular and intercellular pathogen trafficking can take place in the form of viral particles or nucleoprotein complexes and depends on virus encoded polypeptides named movement proteins (MPs). Though there is considerable structural diversity among MPs of distinct virus taxa (Lucas, 2006), functional properties common to most of them can be outlined including nucleic acid binding capacity, interaction with viral and host factors and ability to increment the size exclusion limit of PD (Nelson and Citovsky, 2005; Waigmann et al., 2004). As viruses seem to hijack the cellular machinery of macromolecular transport to promote their own movement, MPs also often associate with host membrane or cytoskeletal elements (Harries et al., 2010). All these activities can be combined in a single MP or be allocated to several MPs that will assist virus spread in a concerted manner (Hull, 2002; Lucas, 2006).

Pelargonium flower break virus (PFBV) is a member of the genus *Carmovirus* in the family *Tombusviridae*. The monopartite single-stranded (ss) RNA genome of PFBV contains five ORFs that encode polypeptides of 27 (p27), 86 (p86), 7 (p7), 12, (p12) and 37 (p37) kDa (Rico and Hernández, 2004). Reverse genetics experiments have indicated that p27 and its readthrough product p86 (the RNA dependent-RNA polymerase), are essential for viral RNA replication while p37 plays a dual role as capsid protein and as suppressor of RNA silencing (Martínez-Turiño and Hernández, 2009, 2010). According to the available data, cell-to-cell transport of carmo-like viruses in plants is aided by two small virus-encoded polypeptides referred to as the double gene block proteins (DGBps; Hull, 2002). In the case of PFBV, DGBp1 and DGBp2 would correspond to p7 and p12, respectively, on the basis of their similarities with carmoviral proteins with assigned movement function (Genovés et al., 2006; Hacker et al., 1992; Li et al., 1998). Structural and molecular studies performed with *Carnation mottle virus* (CarMV) and *Melon necrotic spot virus* (MNSV) have shown that their DGBps1 (CarMV p7 and MNSV p7A) present RNA binding properties mainly mediated by a basic central region that adopts an α-helical conformation in the presence of secondary structure inducers (Marcos et al., 1999; Navarro et al., 2006; Vilar et al., 2001, 2005). Conversely, DGBps2 of these viruses lack RNA binding activity and contain one (MNSV p7B) or two (CarMV p9) transmembrane domains (TMs) that are targeted and inserted *in vitro* into microsomal membranes derived from the endoplasmic reticulum (ER) (Navarro et al., 2006; Vilar et al., 2002). From these findings, a topological model was advanced in which the cytosolic faced-region (s) of the membrane-associated movement protein (DGBp2) would

* Corresponding author. Fax: +34 96 3877859.
E-mail address: cahernan@ibmcp.upv.es (C. Hernández).

0042-6822/$ – see front matter © 2011 Elsevier Inc. All rights reserved.
doi:10.1016/j.virol.2011.03.001

interact with the soluble partner (DGBp1) bound to the viral RNA through their C-terminal regions that might adopt similar β-sheet structures (Navarro et al., 2006; Vilar et al., 2002). The resulting ribonucleotide complex would spread among cells with the aid of an internal membranous translocation system, paralleling that proposed for other MPs (Heinlein and Epel, 2004; Lucas, 2006; Melcher, 2000; Nelson and Citovsky, 2005). As indicated above, this model was mainly based on the properties of DGBps of CarMV and MNSV but *in silico* analyses of the corresponding proteins of other carmoviruses revealed common features that led to the suggestion that the model could apply for most members of the genus (Navarro et al., 2006). Though this was an attractive and straightforward scheme, the mechanism for carmoviral movement is likely more complex and, moreover, virus-specific particularities cannot be discarded. Indeed, most recent results with the DGBps of MNSV have shown that MNSV p7B is targeted *in vivo* to the ER as expected, and delivered to PD via a route that involves the Golgi apparatus (Genovés et al., 2010). However, MNSV p7A is not only able to bind RNA but also to move intracellularly toward PD in the absence of other viral products through a route distinct from that followed by p7B (Genovés et al., 2009). This observation suggests that the distribution of functions among DGBp partners is different or not so well defined as initially proposed.

PFBV p12, like its counterparts in other carmoviruses, contains a high percentage of hydrophobic amino acids distributed along two predicted transmembrane α-helices (Navarro et al., 2006). This trait probably causes the protein to become membrane embedded as described for the homologous CarMV and MNSV proteins and lately for that of *Turnip crinkle virus* (TCV) (Martínez-Gil et al., 2010; Navarro et al., 2006; Vilar et al., 2002). However, several structural peculiarities distinguish PFBV p12 from similar proteins. First, its size is bigger than those of equivalent carmoviral proteins that, with the only exception of the putative DGBp2 of *Japanese iris necrotic ring virus* (Takemoto et al., 2000), range from 7 to 9 kDa (Lommel et al., 2005). Alignment of PFBV p12 with the latter ones indicates that this size gain is primarily due to an N-terminal extension which is rich in basic amino acids (Rico and Hernández, 2004). In addition, p12 contains a seven residue leucine repeat motif, consistent with a leucine zipper, that is absent in related proteins and that is predicted to be four heptads in length (Rico and Hernández, 2004). The natural heterogeneity found among different PFBV isolates argues in favor of the functional relevance of the motif. On one side, only conservative amino acid changes were detected in this region of the molecule and the key leucines of the heptads were strictly preserved despite the large nucleotide variation observed in the corresponding codons (Rico et al., 2006). In addition, an amino acid substitution observed in one isolate would extend the number of heptads of the motif from four to five (Rico et al., 2006).

In order to get insights into the mode of action of PFBV p12, in this work we report experiments aimed at confirming its involvement, together with PFBV p7, in viral movement. We have also investigated the subcellular localization of the protein and the relevance *in vivo* of the putative leucine zipper. Moreover, we have tested whether p12 is endowed with RNA binding activity. Collectively, the results suggest that PFBV p12 may differ mechanistically from related proteins.

Results

Both p7 and p12 are involved in PFBV cell to cell movement

In order to assess whether the two small polypeptides encoded in the central region of PFBV genome, p7 and p12, are involved in viral movement as expected from their homologies with carmoviral proteins of known function (Genovés et al., 2006; Hacker et al., 1992), the start codons of their corresponding ORFs were altered by site-directed mutagenesis using the PFBV infectious clone pSP18F-IC

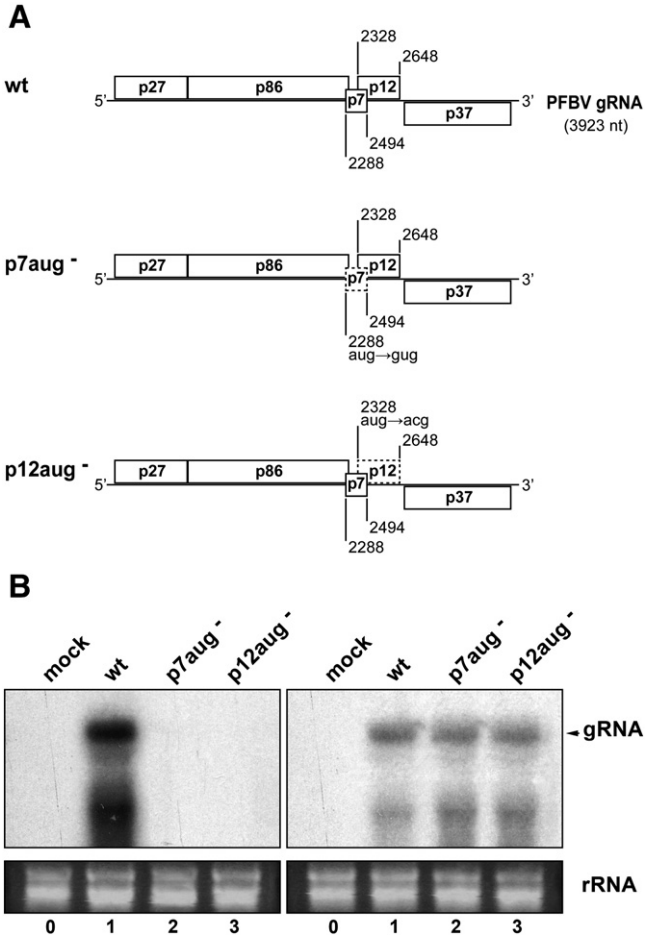

Fig. 1. Bioassay of PFBV mutants. (A) Schematic representation of wt PFBV gRNA (top) and derived mutants p7aug- and p12aug- (bottom). Nucleotide positions of the initiation codons of ORFs p7 and p12 are indicated. Substitutions affecting these codons were introduced into the full-length cDNA clone pSP18-IC leading to triplet changes that are depicted for each mutant. The engineered mutations did not alter the amino acid sequences of overlapping ORFs. In mutants, dashed boxes correspond to ORFs that are not expected to be translated. (B) Northern blot hybridization of total RNA extracted from *C. quinoa* leaves (left panel) or protoplasts (right panel) inoculated with transcripts corresponding to the PFBV wt construct (lane 1) or to mutants p7aug- and p12aug- (lanes 2 and 3, respectively). Lanes 0 correspond to mock-inoculated negative controls. The arrow marks the position of the gRNA; lower bands correspond to subgenomic RNAs. Ethidium bromide staining of rRNA was used as a loading control.

(Rico and Hernández, 2006) as template (Fig. 1A). Run-off transcripts synthesized from the wild type (wt) and the mutated constructs, designated p7aug- and p12aug-, respectively, were used to inoculate *Chenopodium quinoa* leaves and protoplasts. Unlike that observed with the wt construct, no lesions were visible in leaves challenged with the mutant constructs even at 15 days post-inoculation (dpi) and, consistently, no viral-specific signals could be detected by Northern blot hybridization (Fig. 1B). In contrast to that found in plants, mutants p7aug- and p12aug- accumulated in *C. quinoa* protoplasts at levels similar to those of the wt RNA (Fig. 1B). Collectively, the results showed that abolishment of p7 or p12 expression does not affect viral replication but impairs viral spread in leaves supporting the anticipated role of these proteins in cell-to-cell movement.

Amino acid mutations in the leucine zipper-like motif of p12 render movement-defective viruses

To investigate the *in vivo* relevance of the leucine zipper-like motif of p12, nucleotide substitutions leading to single or double replacements of heptadic leucine residues were engineered into the

infectious clone pSP18-IC. The mutations affected either Leu67 (mutants LZM1 and LZM2 with the amino acid substitutions Leu67Ile and Leu67Ala, respectively), Leu81 (mutants LZM3 and LZM4 with the amino acid substitutions Leu81Arg and Leu81Ala, respectively), or both simultaneously (mutants LZM5, with changes Leu67Ile and Leu81Arg, and LZM6, with changes Leu67Ala and Leu81Ala) (Fig. 2A). The replacement Leu67 by Ile and Leu81 by Arg was based on the presence of such amino acid residues at equivalent positions of homologous proteins (Rico and Hernández, 2004). On the other hand, Ala was chosen over other amino acids as a substituting residue of the heptadic leucine residues because of the fact that Ala has a strong propensity to form an α-helix and its substitution has been documented to have minimal disruptive effects on the alpha-helical structure characteristic of a leucine zipper domain (Lyu et al., 1990; O'Neil and DeGrado, 1990; Zhang et al., 1991). In addition, Ala lacks the bulky hydrophobic side chain of a leucine residue, which is believed to be the major hydrophobic force for a leucine zipper domain to facilitate protein interaction (O'Shea et al., 1989). Thus, replacement of heptadic leucine residues by alanine would likely influence only the biological properties derived from the bulky hydrophobic side chain of a leucine residue while having minimal effects on the overall alpha-helical structure. Transcripts derived from the wt and mutant clones were used to inoculate *C. quinoa* plants. As opposed to wt RNA, none of the mutants induced appearance of chlorotic lesions on the inoculated leaves and a Northern blot analysis confirmed the absence of PFBV in this plant material (Fig. 2B, upper panel). Two control mutants were additionally generated, one with the putative leucine zipper extended in one heptad (change Ser53Leu) and the other harbouring an amino acid replacement outside of the leucine zipper-like motif (Gly14Glu) as found, respectively, in one and nineteen natural isolates of the virus (Rico et al., 2006). These mutants were fully infectious in *C. quinoa* (data not shown) denoting that the results observed through alteration of critical residues of the leucine zipper motif were sequence-specific and not a side effect of the mutagenesis. In order to eliminate the possibility that the nucleotide substitutions engineered in constructs LZM1 to LZM6 disrupted *cis*-acting elements essential for replication, these constructs were transfected in *C. quinoa* protoplasts. Northern blot analysis revealed that all assayed mutants accumulated to levels equivalent to those of the wt RNA (Fig. 2B, lower panel), indicating that their incapacity to establish effective infections in plants was due to a defect in movement rather than to a blockage in viral replication. Overall, the data support the conclusion that the leucine zipper-like motif is critical for the movement function of p12.

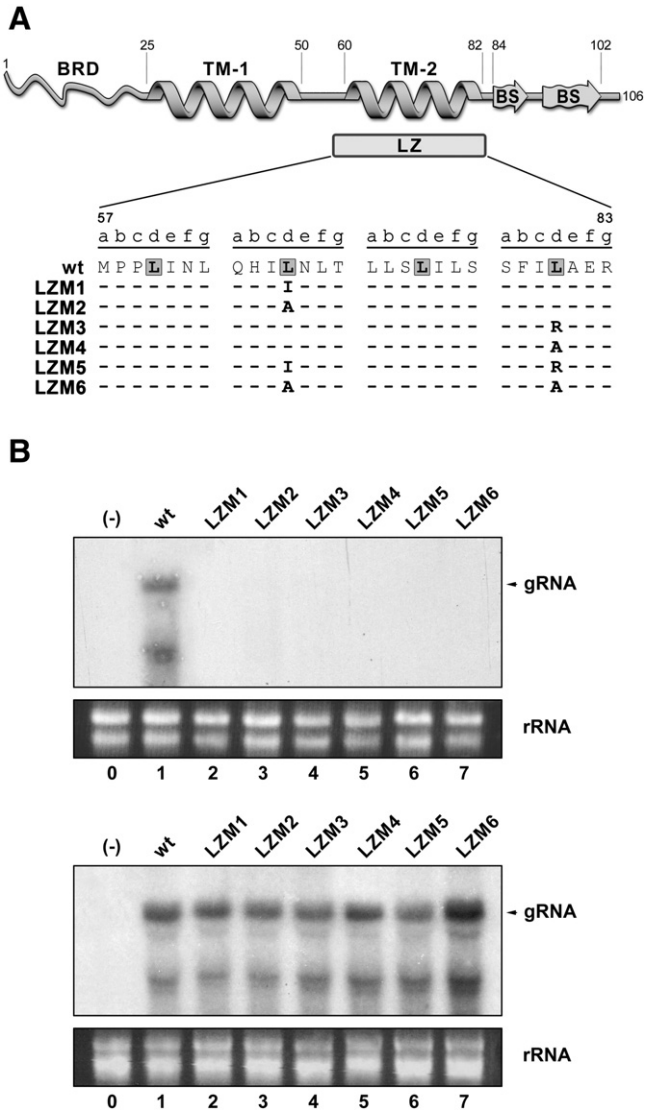

Fig. 2. Effect of amino acid substitutions in the leucine zipper-like domain of p12 on virus infection. (A) *Top*. Schematic diagram of p12 showing the relative location of the putative leucine zipper motif (LZ) in relation to other predicted domains of the protein. Boundaries of each domain are indicated. BRD: domain at the N-terminus rich in basic amino acids; TM: stretch of residues predicted to be involved in α-helix or transmembrane segments; LZ: leucine zipper-like domain; BS: β-sheet structured region. *Bottom*. Aminoacid sequence of the leucine zipper-like motif in wt and mutant constructs. Dashed lines represent residues identical to the wt protein whereas specific amino acid replacements are indicated for each mutant. The seven positions of the heptad repeat are labeled "a" through "g". The residues found at critical "d" positions are highlighted in boldface type. (B) Northern blot hybridization of total RNA extracted from plants (upper panel) or protoplasts (lower panel) inoculated with transcripts corresponding to the PFBV wt construct (lane 1) or mutants LZM1 to LZM6 (lanes 2 to 7) as indicated above the lanes. Lanes 0 correspond to buffer-inoculated negative controls. The arrow marks the position of the genomic RNA; lower bands correspond to subgenomic RNAs. Ethidium bromide staining of rRNA was used as a loading control.

p12 mainly localizes to the ER and is recovered in membranous fractions

As indicated above, computer analysis of p12 sequence predicted that it is a membrane protein with two TMs that roughly span from residues 25 to 50 and 60 to 82, respectively (Fig. 2A). To investigate potential association of p12 to cellular membranes, this PFBV product was fused to the green fluorescent protein (GFP) and transiently expressed in *Nicotiana benthamiana* leaves via agroinfiltration. Whereas expression of free GFP gave the typical diffuse green fluorescence evenly distributed through the cytoplasm and the nucleus, fluorescence derived from the fusion p12GFP labelled an intracellular reticulate network likely corresponding to the ER (Fig. 3, panels A and B). To confirm this issue, p12 was fused to the monomeric red fluorescent protein (mRFP) and delivered by agroinfiltration into transgenic 16c *N. benthamiana* plants expressing ER-targeted GFP (GFP-KDEL, Ruiz et al., 1998). A perfect match among the p12mRFP and GFP-KDEL fluorescent signals was observed thus corroborating that p12 localizes mainly to the ER (Fig. 3, panels D to F). Nevertheless, sorting of the protein to other cellular membranes cannot be excluded since the green fluorescence of the p12GFP fusion was occasionally observed in punctuate structures at the cytoplasm and close to the plasma membrane (Fig. 3, panel C and data not shown). Interestingly, the pattern of cytoplasmic punctuate structures strongly resembled the motile bodies formed by MNSV p7b at the Golgi stacks (Genovés et al., 2010). Consistent with these general observations, subcellular fractionation and Western blot analysis of proteins extracted from GFP- and p12GFP-expressing plant tissue revealed the presence of the fused product in the pellet fraction (P30) following centrifugation at 30.000×*g*, in contrast to the unfused GFP that, as expected, was recovered in the supernatant (S30) (Fig. 3G). Because the P30

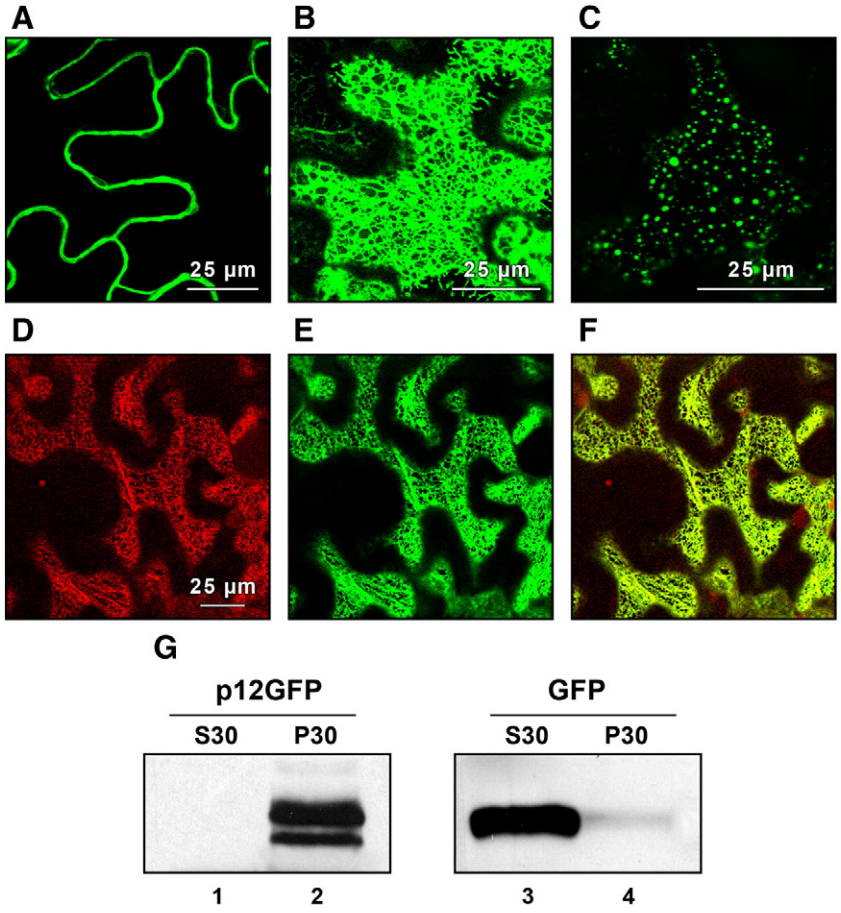

Fig. 3. Studies on the subcellular localization of PFBV p12 in *N. benthamiana* leaves through transient expression. (A to C) Confocal scanning microscopy analysis of non- transgenic *N. benthamiana* leaves expressing unfused GFP (A, green channel) or the p12GFP fusion (B and C, green channel). (D to F) Confocal scanning microscopy analysis of leaves from transgenic 16c *N. benthamiana* plants expressing an ER-targeted GFP (Ruiz et al., 1998), after agroinfiltration with the construct that allows translation of the p12mRFP fusion. D and E display images through the red and green channel, respectively, and F corresponds to an overlay. (G) Immunoblot analysis, using anti-GFP antibody, of protein extracts from GFP- and p12GFP- expressing *N. benthamiana* leaves (right and left blots, respectively). S30 (lanes 1 and 3) and P30 (lanes 2 and 4), supernatant and pellet, respectively, following centrifugation at 30,000×*g*.

fraction contains membrane-derived microsomes, we can conclude that p12 is indeed a membrane-associated protein.

p12 has RNA binding activity

Positively charged amino acids are frequently involved in nucleic acid binding properties of proteins (Chen and Varani, 2005; Weiss and Narayana, 1998). As mentioned previously, PFBV p12 contains a specific N-terminal extension which is rich in basic amino acids (Fig. 2A). This structure prompted us to explore whether this protein could be endowed with RNA binding activity, which would differ from that reported for the equivalent product of MNSV or postulated for other DGBps2 (Navarro et al., 2006; Saurí et al., 2005). To this aim, a recombinant p12 fused to a His-tag was expressed in *E. coli* and purified by chromatography on Ni-NTA columns. Despite the known difficulties associated to production and purification of hydrophobic, membrane proteins in bacteria (Luan et al., 2004), we were able to obtain sufficient amounts for biochemical studies. In order to improve protein solubility, Arg and Glu were added at 50 mM to the storage buffer which had a positive effect in preventing protein aggregation and precipitation and increased the long-term stability of the sample, in line with that described for diverse proteins (Golovanov et al., 2004). Electrophoretic mobility shift assays (EMSAs) were performed with increasing quantities of the recombinant protein and a ^{32}P-labeled ssRNA probe (5′-PFBV) encompassing the 5′-terminal 140 nt of PFBV genome. RNA mobility shift, suggesting the presence of an RNA protein-interaction, became detectable when the His-tagged p12 was added at a concentration of 0.21 μM to the reaction mixture. Complete retardation of the probe was observed at 13.10 μM and at higher concentrations, as measured by disappearance of unbound RNA (Fig. 4A). Treatment of the preparation of purified p12 with proteinase K before adding the RNA probe prevented formation of the retarded band confirming that the shift resulted from the interaction of the RNA with the protein (data not shown). Furthermore, when the His-tagged p12 was replaced by bovine serum albumin (BSA) in control gel shift assays, no retardation of the probe was observed indicating that the association between p12 and the ssRNA was not an artefact of the specific experimental conditions employed (Fig. 4A, lane 10). Non-linear regression of the binding data (Fig. 4B) allowed estimating an apparent K_d of 3.14 μM, which was in the range of those reported for distinct viral RNA binding proteins including several MPs (Daròs and Carrington, 1997; Herranz and Pallás, 2004; Marcos et al., 1999; Navarro et al., 2006; Skuzeski and Morris, 1995). Only two forms of the probe were detectable in the EMSA assays, free RNA and completely retarded complex with no obvious intermediate shifted bands, which would suggest a cooperative binding of p12 to ssRNA (Citovsky et al., 1990). However, the slope of the best-fit curve (h or Hill slope) for the binding data, calculated from three independent experiments, was found to be 1 lending little support to a cooperative view of the protein:RNA interaction ($h=1$ is indicative of non-cooperative binding and $h>1$ is an indication of positive cooperative binding). It is worth mentioning in this context that attempts to further concentrate our protein preparation without affecting stability were unsuccessful, which precluded more detailed characterization of the binding kinetics.

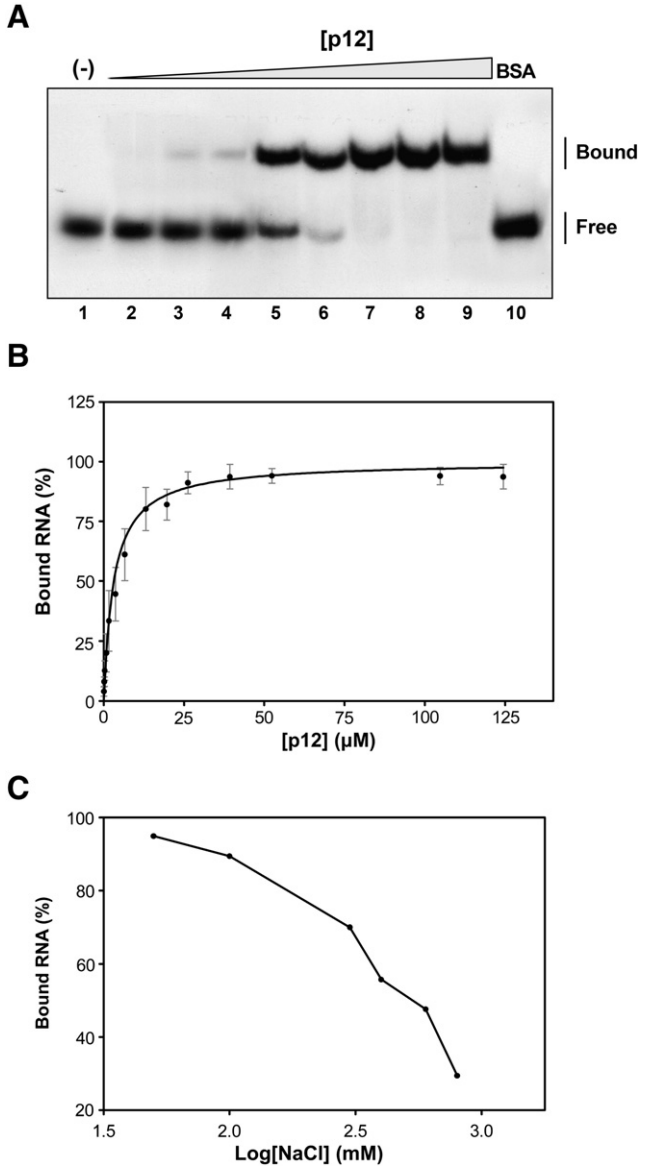

Fig. 4. Analysis of RNA-binding properties of PFBV p12 *in vitro*. (A) Representative EMSA showing interactions between the recombinant p12 and ssRNA. The ^{32}P-labeled 5′-PFBV ssRNA probe (at 97 pM) was incubated with no protein (lane 1) or with His-tagged p12 at 0.10, 0.21, 0.33, 3.70, 6.55, 13.10, 26.20 and 52.41 μM (lanes 2 to 9, respectively). The unbound, free RNA probe and the shifted (bound) RNA complexes are marked on the right. (B) Best-fit curve of the binding data from three independent experiments determined by non-linear regression. (C) Effect of NaCl concentration on the RNA binding activity of PFBV p12. The fraction of bound ssRNA was plotted against the log[NaCl] (in mM) to estimate the IC_{50} value.

To investigate how the RNA-binding ability of p12 was dependent on electrostatic interactions, EMSAs were performed using increasing NaCl concentrations in the incubation mixtures. An amount of protein that was sufficient to bind all RNA molecules was employed (40.0 μM) and, thus, the appearance of free RNA was quantified to evaluate complex dissociation (Fig. 4C). The NaCl concentration at which binding was reduced to 50% of maximal levels (IC_{50}) was 525 mM, a remarkable salt tolerance that, nevertheless, was in the range of those determined for other RNA-binding proteins of viral origin (Brantley and Hunt, 1993; López et al., 2000; Marcos et al., 1999; Martínez-Turiño and Hernández, 2010; Navarro et al., 2006; Richmond et al., 1998). These results suggested that electrostatic interactions are not the only ones involved in binding of p12 to the RNA.

p12 is a non-sequence specific ssRNA binding protein

Competition experiments were performed to examine the binding selectivity of p12. For this purpose, unlabeled nucleic acids corresponding to either ssRNA, double- stranded (ds) RNA, ssDNA or dsDNA molecules were added to the binding mixtures at 1-, 10- and 100-fold molar excess over the radiolabeled probe. In the case of ssRNA, two distinct competitors were used, one derived from the 3′-terminal region of the PFBV genome (3′PFBV-ssRNA) and the other from a heterologous source (het-ssRNA). Fixed amounts of His-tagged p12 (32.75 μM) and ^{32}P-labeled 5′-PFBV probe (97.0 pM), that resulted in more than 99% of the ssRNA bound to the protein, were used in the binding reactions. EMSAs revealed that dsRNA and dsDNA were poor competitors because a major fraction of the probe remained bound to p12 even at a 100 molar excess (Fig. 5). At the same molar excess, the ssDNA behaved as moderately good competitor as the binding of p12 to the probe was significantly affected (Fig. 5). However, ssRNAs were undoubtedly the best competitors irrespectively of their origin, as they completely prevented formation of the p12:probe complex when added at the greatest concentration (Fig. 5). Overall, the data indicated that p12 is a single-stranded nucleic acid-binding protein with the highest preference toward any ssRNA.

p12 RNA binding is attributable to its basic N-terminal domain

In order to map the region of p12 responsible of its binding activity, the N- or C-terminal region of the molecule was removed to create two truncated forms of the protein, p12(26–106) and p12(1–59). In addition, several mutated versions of p12(1–59) were generated by consecutively replacing Arg residues of the N-terminal region by Ala. The mutants were designated as p12(1–59)m2R (carrying substitutions Arg16Ala and Arg17Ala), p12(1–59)m3R (carrying substitutions Arg16Ala, Arg17Ala and Arg19Ala) and p12(1–59)m4R (carrying substitutions Arg16Ala, Arg17Ala, Arg19Ala and Arg24Ala) (Fig. 6A). All p12 derivatives were expressed in *E. coli* as His-tagged fusions, purified by chromatography on Ni-NTA columns and subjected to Northwestern assay to evaluate RNA-binding capability. To this aim, equivalent amounts of the purified proteins were separated, together with the wt p12, by SDS-PAGE and subsequently transferred to a nitrocellulose membrane. After a renaturation step, the membrane was incubated with ^{32}P-labeled 5′-PFBV ssRNA probe. A signal was detected in the position corresponding to the full-length protein (Fig. 6B) which was in accordance with the EMSA results and ruled out the possibility that any contaminating protein(s) from *E. coli* could account for the observed RNA binding activity. Remarkably, a similar, or even stronger, signal was noticed in the position of p12(1–59) whereas no signal was present in the portion of the membrane that contained p12(26–106). These results strongly suggested that the RNA binding properties of p12 could be provided by its N-terminal basic extension. Consistent with this possibility, double replacement of Arg by Ala in this domain strongly diminished the binding capability of p12(1–59) (protein p12[1–59]m2R; Fig. 6B) which was reduced to negligible levels when one or two additional Arg residues were mutated (proteins p12[1–59]m3R and p12[1–59]m4R, respectively; Fig. 6B). These results confirmed the involvement of the N-terminal region in the binding activity of p12 and, moreover, highlighted the contribution of positively charged amino acids to such activity.

Discussion

Here, we have corroborated the requirement of the two small, centrally encoded PFBV proteins, p7 and p12, for virus movement. Computer analyses suggest that PFBV p7 structure fits well with the general scheme proposed for carmoviral DGBp1 that distinguishes three different structural domains: an unordered N-terminus, an α-

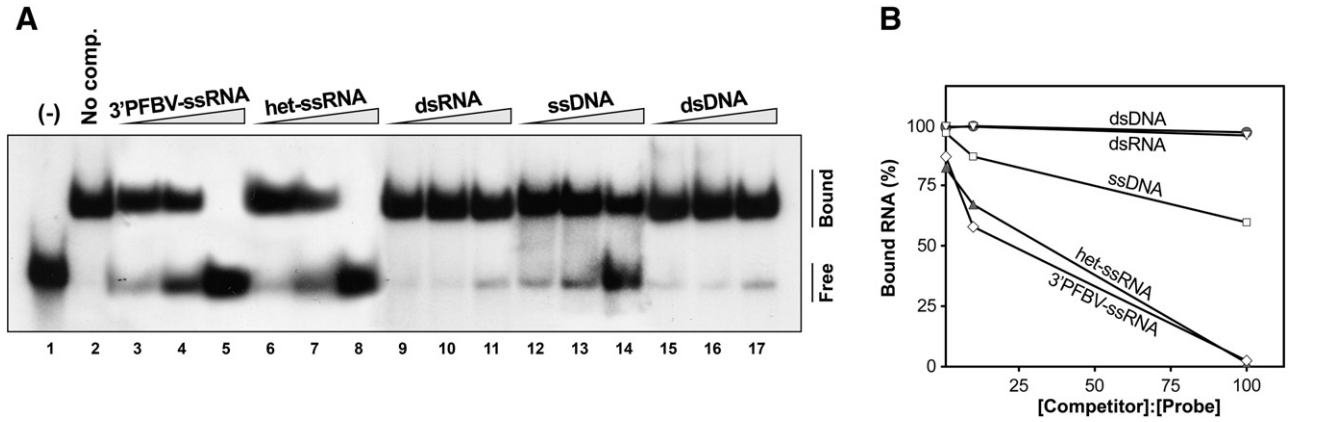

Fig. 5. Competition assays to evaluate binding specificity of p12. (A) EMSAs performed after incubation of His-tagged p12 (32.75 μM) and ^{32}P-labeled, 5′-PFBV ssRNA probe (at 97.0 pM) in the absence (lane 2) or the presence (lanes 3 to 17) of increasing amounts (1, 10- and 100-fold molar excess) of unlabeled competitors as shown at the top of the autoradiograms. Lanes 1, no protein. (B) Graphical representation of the EMSA results. The percentage of free probe has been plotted against competitor/probe molar ratio. The experiments were repeated twice with essentially identical results (data of one set of experiments are presented here).

helical central region and a C-terminus with potential β-sheet folding (Akgoz et al., 2001; Marcos et al., 1999; Navarro et al., 2006; Vilar et al., 2001, 2005). The central region is rich in positively charged amino acids and is expected to endow the protein with RNA binding properties as it has been demonstrated for CarMV and MNSV DGBp1 (Marcos et al., 1999; Navarro et al., 2006) as well as the corresponding product of *Turnip crinkle virus* (Wobbe et al., 1998). According to *in silico* evaluations, PFBV p12 shares also main features with related products including a C-terminal region with likely β-sheet folding and the presence of two transmembrane domains. Consistent with the latter prediction, the protein was recovered in membranous fractions and it was found to localize mainly to the ER, paralleling that reported for homologous and non-homologous MPs (Genovés et al., 2010; Heinlein et al., 1998; Ju et al., 2005; Peremyslov et al., 2004; Schepetilnikov et al., 2008). Nevertheless, as PD is most probably the final target of p12, interaction of the protein with other components of the cellular macromolecular transport system at different stages of infection cannot be ruled out. This possibility was indeed suggested by some localization patterns of p12 (Fig. 3, panel C and data not shown) and, if confirmed, it would be in line with that reported for MNSV p7B and for distinct MPs (Genovés et al., 2010; Haupt et al., 2005; Heinlein et al., 1998). Despite the above similarities, PFBV p12 differs from other carmoviral DGBps2 in having a basic N-terminal extension and a leucine zipper-like motif. This prompted us to investigate potential functional implications of these PFBV p12-particular traits.

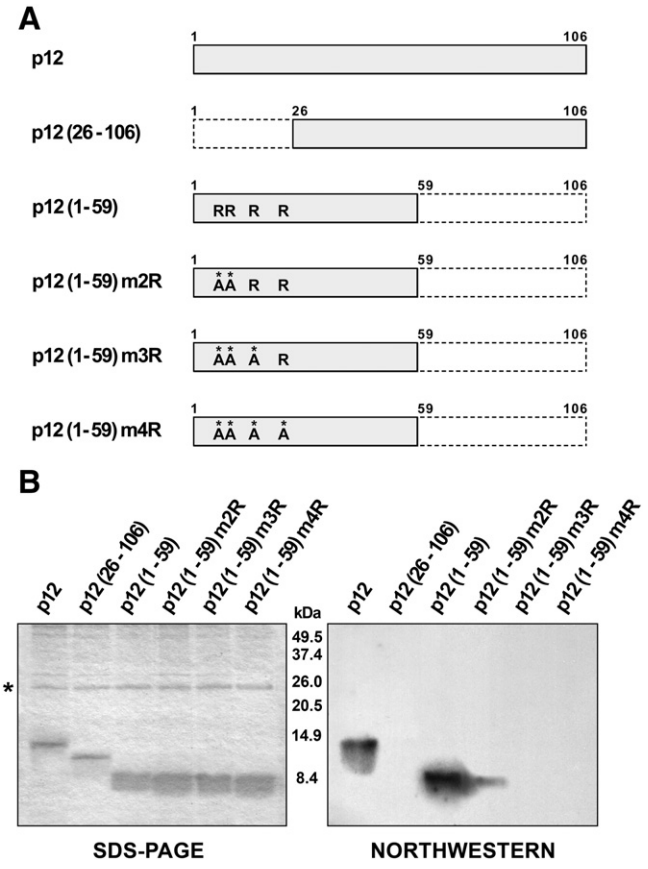

Fig. 6. Mapping the RNA binding domain of p12. (A) Schematic representation of p12 and its mutant forms, p12(26–106), p12(1–59), p12(1–59)m2R, p12(1–59)m3R, p12 (1–59)m4R. Dashed lines indicate deleted regions in the truncated forms. In mutant versions, replacement of arginine residues by alanines are indicated. (B) Northwestern analysis of p12 and mutated forms. The purified recombinant proteins were separated by SDS-15% PAGE as shown in the left panel after Coomasie blue staining, and transferred to a nitrocellulose membrane that was incubated with the ^{32}P-labeled ssRNA probe (5′-PFBV) and autoradiographed as shown in the right panel. The asterisk in the left panel marks the position of a non-specific protein band.

Leucine zippers are known to engage in protein-protein interactions and are composed of a heptad repeat of amino acids (Busch and Sassone-Corsi, 1990; Landschulz et al., 1998). This type of motifs adjust frequently to the "abcdefg rule" that holds that positions "a" and "d" of the heptad are occupied by hydrophobic amino acids while positions "e" and "g" are occupied by charged amino acids. Though this rule is usually met by "classical" leucine zipper motifs, numerous modified leucine zippers that show lax adherence to the rule but preserve their function as intermolecular clamps have been described (e.g: Chevalier et al., 2008; Fry et al., 1999). In many cases, however, the presence of leucine residues at positions "d" has been found to be critical (Bornberg-Bauer et al., 1998; Moitra et al., 1997). The putative leucine zipper of PFBV p12 deviates to some extent from the classical structure (Fig. 2) but the strict conservation of the motif and, particularly, of the key leucines in all isolates of the virus characterized so far (Rico et al., 2006) suggested it could be relevant for the functionality of the protein. Supporting this view, single and double alterations of pivotal leucines rendered p12 mutants unable to aid viral movement. Most likely, the engineered amino acid substitutions precluded essential association(s) of p12 with itself and/or with proteins of distinct nature. The involvement of leucine zipper motifs in homo and/or heterodimerization has been reported in both animal and plant viruses. Examples of the latter ones include the interaction

between the aphid transmission factor and the virion-associated protein of *Cauliflower mosaic virus* (Leh et al., 2001), or the self-interaction of the ORF II-encoded product of *Soybean chlorotic mottle virus* (Takemoto and Hibi, 2005). We have tried to search for p12 interacting proteins through the split-ubiquitin membrane two-hybrid assay (Fetchko and Stagljar, 2004) but our attempts have been unsuccessful as p12 used as bait caused activation of the reporter in the absence of prey proteins. Assessment of potential p12 homodimerization through bimolecular fluorescence complementation (BiFC) has neither yielded clear results (data not shown). Other approaches will be needed to investigate formation of hydrophobic bonds among the leucine zipper of p12 and other leucine zipper partners. Interestingly, a host homeodomain leucine zipper protein has been found to interact with the MP of a related virus, *Tomato bushy stunt virus* (genus *Tombusvirus*, family *Tombusviridae*), an interaction that correlated with the movement activity of the protein (Desvoyes et al., 2002). Whether this factor and/or different ones are recruited by p12 for directing viral transport remains to be seen. It is also worth mentioning that leucine zippers have been implicated in some instances in regulation of post-translational modification(s) rather than in promotion of protein-protein interactions (Long et al., 2008; Pagano et al., 2009). Such type of modifications might play an important role in MP activity (Kawakami et al., 2003). Several phosphorylation and glycosylation sites are predicted in p12 (data not shown). We can thus not exclude that mutations introduced in its leucine zipper-like motif have not a direct effect on association of the protein with specific viral/host factors but instead provoke conformational changes that prevent post-translational modifications required for modulation of its activity.

The other peculiarity of PFBV DGBp2 concerns to its size increment when compared with homologous proteins, an increment that results from the presence of an N-terminal extension. Abolishment of the initiation codon of ORF p12 in mutant p12aug- might still allow translation from the downstream ^{2424}AUG which would led to production of a truncated protein with a predicted size (8.5 kDa) resembling more those of other DGBps2 (Navarro et al., 2006). The lack of infectivity of this mutant in plants supports that the N-terminus of p12 is absolutely required during the virus life cycle. Outstandingly, we have shown that, unlike related proteins, PFBV p12 possesses RNA binding activity and, moreover, that this activity is provided by its N-terminal region. Basic residues of this region have been shown to play an essential role in RNA binding as mutation of just two arginine residues strongly reduced the capability of the protein to interact with the RNA and this capability was virtually abolished by mutation of further arginines (Fig. 6). These results are in agreement with those reporting the main participation of positively charged amino acids in RNA binding activity of diverse viral proteins (Ansel-McKinney et al., 1996; Genovés et al., 2009; Herranz and Pallás, 2004; Martínez-Turiño and Hernández, 2010; Rao and Grantham, 1996; Wobbe et al., 1998). In addition, the *in vitro* studies have revealed that PFBV p12, as other MPs (Brill et al., 2000; Herranz and Pallás, 2004; Navarro et al., 2006), has a preference for single-stranded nucleic acids, particularly to ssRNA that apparently binds in a sequence non-specific manner. Sequence specificity *in vivo* is likely afforded through other viral- and/or host-coded proteins. Alternatively, compartimentalization of viral components could preclude the protein from association to and movement of cellular RNAs. It is also noteworthy that, according the estimated K_d (3.14 μM), the affinity of p12 for ssRNA is similar to that determined for carmoviral DGBps1 like CarMV p7 and MNSV p7A (1.1 μM and 25.7 μM, respectively; Marcos et al., 1999; Navarro et al., 2006), suggesting that this p12 activity is not marginal or secondary but relevant during the infectious process.

To conclude, we have proven the requirement of the leucine zipper-like motif and of the N-terminal extension of PFBV p12 for effective viral infection. We do not know at this stage which particular conditions have driven the evolution of such specific traits. We can speculate that the answer to this issue is related with the adaptation of the virus to its narrow host range as PFBV is restricted to *Pelargonium* spp. in nature. Significant examples of carmovirus adaptation, including PFBV, to a particular host have been described (Liang et al., 2002a; Rico et al., 2006). Remarkable in this context is the finding that *Hibiscus chlorotic ringspot virus* encodes a protein (p23) that has no homologs in other carmoviruses and that confers host specificity. Curiously, such a protein, as PFBV p12, contains a putative leucine zipper though the biological significance of the motif has yet to be explored (Liang et al., 2002b). On the other hand, the present study raises new questions on the role(s) of the DGBp partners during virus movement. As mentioned in the Introduction section, recent results suggest that MNSV DGBp1 cannot only bind the viral genome but probably has also the capacity to transport it toward PD following a route different from that used by MNSV DGBp2 (Genovés et al., 2009, 2010). The role of the latter protein would then be uncertain but it could be related with PD gating rather than with the intracellular movement of the DGBp1-genome complex as initially proposed. In the case of PFBV, the RNA binding ability of DGBp2 and, most likely, of DGBp1 could provide an additional advantage to the virus by potentially increasing the number of viral genomes that can reach and pass through the intercellular connections, thus facilitating the spread of the pathogen. Additional work might provide further clues on this attracting possibility.

Materials and methods

Generation of constructs

Site-directed mutations affecting ORFs p7 and p12 were introduced into the PFBV infectious clone pSP18-IC (Rico and Hernández, 2006) by PCR using with the Quick Change Site-Directed Mutagenesis kit (Stratagene) and proper oligonucleotide pairs. The mutations altered the presumed start codons of each ORF or led to amino acid replacements in selected regions of p12.

Binary constructs for transient expression in plants were generated as follows. ORF p12 was PCR amplified from the infectious clone pSP18-IC using specific primer pairs and the Expand High Fidelity PCR System (Roche). The amplification product, bearing proper restriction sites at the ends, was fused in frame to the 5′ end of the GFP or monomeric (m) RFP genes by standard cloning procedures (Sambrook et al., 2007). The unfused GFP gene and the DNA fusions p12GFP and p12mRFP were inserted between the *Cauliflower mosaic virus* (CaMV) 35S promoter and the terminator sequence of the *Solanum tuberosum* proteinase inhibitor II gene (PoPit) and cloned into the binary vector pMOG800 (Knoester et al., 1998) to yield constructs pMOG-GFP, pMOG-p12GFP and pMOG-p12mRFP, respectively.

A similar approach was followed to obtain constructs for protein expression in *E. coli*. Full-length and truncated forms of ORF p12 were PCR amplified and cloned into the pET-23d(+) vector (Novagen) through its *Nco*I and *Hind*III restriction sites. The resulting recombinant plasmids, named pET-p12, pET-p12(1–59) and pET-p12(26–106), contained the corresponding version of the PFBV gene fused to a sequence coding for a hexa-histidine tag. Three additional constructs, pET-p12(1–59)m2R, pET-p12(1–59)m3R and pET-p12(1–59)m4R, identical to pET-p12(1–59) but with nucleotide substitutions that led to the replacement of two, three and four arginine residues by alanines, respectively, in the corresponding proteins were generated by PCR with the Quick Change Site-Directed Mutagenesis kit (Stratagene). All constructs were routinely sequenced with an ABI PRISM DNA sequencer 377 (Perkin-Elmer) to avoid unwanted modifications. The primers used to generate the distinct plasmids are listed in Table 1. Representation of the type and specific position of the modifications introduced in each mutant construct is shown in the corresponding figures.

Table 1
List of primers used in this work.

Primer	Position[a]	Sequence[b]		Construct
CH349	2276-2303 (S)	5′ CCACACAATTGAgTGGCTTCTAAAGTGA-3′		p7aug-
CH350	2276-2303 (AS)	5′-TCACTTTAGAAGCCAcTCAATTGTGTGG-3′		
CH79	2317-2342 (S)	5′-GGGTAGTGATAAcGAGATTGACGTGC-3′		p12aug-
CH80	2317-2342 (AS)	5′-GCACGTCAATCTCgTTATCACTACCC-3′		
CH81	2516-2540 (S)	5′-CCAACACATAaTcAATCTTACCTTG-3′		LZM1
CH82	2516-2540 (AS)	5′-CAAGGTAAGATTgAtTATGTGTTGG-3′		LZM5
CH83	2514-2537 (S)	5′-CTCCAACACATAgcGAATCTTACC-3′		LZM2
CH84	2514-2537 (AS)	5′-GGTAAGATTCgcTATGTGTTGGAG-3′		LZM6
CH85	2557-2580 (S)	5′-GTTCTTTCATCcgGGCAGAGAGAG-3′		LZM3
CH86	2557-2580 (AS)	5′-CTCTCTCTGCCcgGATGAAAGAAC-3′		LZM5
CH87	2557-2580 (S)	5′-GTTCTTTCATCgcGGCAGAGAGAG-3′		LZM4
CH88	2557-2580 (AS)	5′-CTCTCTCTGCCgcGATGAAAGAAC-3′		LZM6
CH39	2328-2347 (S)	5′-GGGGGATCCATGAGATTGACGTGTCAGTG-3′	(*BamH*I)	pMOG-p12GFP
CH38	2626-2645 (AS)	5′-GGAAGCTTAGGATCCTTGCCCAGTTGAGATCCGTA-3′	(*BamH*I)	pMOG-p12mRFP
DH5P12	2328-2351 (S)	5′-GGCCATGGGATTGACGTGTCAGTGGGAG-3′	(*Nco*I)	pET-p12
CH69	2625-2645 (AS)	5′-CCAAGCTTTTGCCCAGTTGAGATCCGTAT-3′	(*Hind*III)	
DH5P12	2328-2351 (S)	5′-GGCCATGGGATTGACGTGTCAGTGGGAG-3′	(*Nco*I)	pET-p12(1–59)
CH96	2482-2504 (AS)	5′-CCAAGCTTAGGGGGCATACTAAAAGTTGAAG-3′	(*Hind*III)	
CH265	2401-2423 (S)	5′-GGCCATGGCGCTGTCTCCAAACGGACATCTG-3′	(*Nco*I)	pET-p12(26–106)
CH69	2625-2645 (AS)	5′-CCAAGCTTTTGCCCAGTTGAGATCCGTAT-3′	(*Hind*III)	
CH300	2359-2391 (S)	5′-GAATAGGGGGAAACgcAgcGGTAAGATATCCGT-3′		pET-p12(1–59)m2R
CH301	2359-2391 (AS)	5′-ACGGATATCTTACCgcTgcGTTTCCCCCTATTC-3′		
CH302	2370-2396 (S)	5′-AACgcAgcGGTAgcATATCCGTCGCAA-3′		pET-p12(1–59)m3R
CH303	2370-2396 (AS)	5′-TTGCGACGGATATgcTACCgcTgcGTT-3′		
CH304	2385-2411 (S)	5′-TATCCGTCGCAAgcGACGCTGTCTCCA-3′		pET-p12(1–59)m4R
CH305	2385-2411 (AS)	5′-TGGAGACAGCGTCgcTTGCGACGGATA-3′		

[a] Positions of the PFBV genome covered by the primers. (S) and (AS): sense and antisense.
[b] Restriction sites introduced for cloning purposes are underlined and lowercase indicate nucleotide substitutions to PFBV wt sequence.

Inoculation of plants and protoplasts

Transcripts were synthesized *in vitro* from wt clone pSP18-IC and derived mutant constructs with T7 RNA polymerase (Fermentas) following digestion of plasmids with *Xba*I. Protoplasts (0.5×10^6), prepared from *C. quinoa* leaves (Hans et al., 1992), were inoculated with 10 μg of PFBV genomic transcripts by using polyethylene glycol. The same type of transcripts was used to mechanically inoculate *C. quinoa* plants (three leaves per plant employing approximately 2 μg of transcript per leave). Plants were maintained under greenhouse conditions (16 h days at 24 °C, 8 h nights at 20 °C) and monitored for lesion appearance from 7 to 15 dpi.

RNA extraction and Northern blot hybridization

Total RNA preparations from *C. quinoa* leaves were obtained by phenol extraction and lithium precipitation (Verwoerd et al., 1989). In addition, total RNA was extracted from protoplast samples using TRI Reagent according the manufacturers instructions (SIGMA). Northern blot analysis was performed with a ^{32}P-radioactive DNA probe, derived from the 3′ region of PFBV genome, as previously described (Rico and Hernández, 2009).

Agrobacterium-mediated transient expression, subcellular fractionation and immunoblotting

For transient expression in plants, constructs pMOG-GFP, pMOG-p12GFP and pMOG-p12mRFP were used to transform *Agrobacterium tumefaciens* strain C58C1 (pCH32). Transformed bacteria were grown overnight in proper conditions and subsequently collected by slow-speed centrifugation and adjusted to the required final OD_{600} (0.5) value with 10 mM $MgCl_2$, 10 mM MES, pH 5.6 and 150 μM acetosyringone. After 2 h incubation, the suspensions were infiltrated with a 5 ml needleless syringe on the abaxial side of leaves from 3-week-old *N. benthamiana* plants as previously described (Martínez-Turiño and Hernández, 2009).

To prepare soluble and insoluble fractions from GFP and p12GFP-expressing plant tissue, *N. benthamiana* leaves were collected 5 days after agroinfiltration with the corresponding construct and ground with a mortar and pestle with 5 ml of extraction buffer (50 mM Tris-acetate, pH 7.4, 10 mM potassium acetate, 1 mM EDTA, 5 mM dithiothreitol, 0.5 mM phenylmethylsulfonyl fluoride) per g of fresh weight. After extraction, the homogenates were centrifuged at $3{,}000\times g$ for 10 min to remove large cellular debris and the resulting supernadant was ultracentrifuged at $30{,}000\times g$ for 1 h to generate the soluble (S30) and the microsomal (P30) fractions. Then, the P30 fraction was resuspended in 500 μl of extraction buffer. The S30 and P30 fractions were electrophoresed, transferred to polyvinylidene fluoride membranes (PVDF) membranes (Roche) and immunoblotted with anti-GFP (Roche). Immunoreactive bands were revealed with chemiluminescence ECL Plus kit following supplier recommendations (GE Healthcare).

Fluorescence microscopy

A Leica TCS SL confocal microscope was used to obtain images employing an HCX PL APO×40/1.25-0.75 oil CS objective. GFP fluorescence was monitored by excitation with 488 nm argon laser line with emission being collected through band-pass filter from 505 to 550 nm. In the case of mRFP, excitation was performed by means of a 543-nm green-neon laser line, and fluorescence emission was collected at 610 to 630 nm. Observation of fluorescence in agroinfiltrated *N. benthamiana* leaves was done at 48–72 h post-infiltration.

Expression and purification of PFBV p12 and derivatives

The pET-23d(+)-based constructs were used to transform *E. coli* Rosetta (DE3)pLysS (Novagen). Expression of the His-tagged p12 protein and derivatives was induced in the transformed bacteria with isopropyl-b-D-thiogalactopiranoside (IPTG) at 0.4 mM for 4 h at 37 °C. Purification of the proteins was performed by metal affinity chromatography in denaturing conditions using nickel-nitrilotriacetic acid (Ni-NTA) columns and following manufacturer recommendations (Sigma). His-tagged proteins were finally eluted from the columns in a buffer containing 500 mM imidazole, 300 mM NaCl and 50 mM NaH_2PO_4/Na_2HPO_4, pH 8.0. Purified preparations were

dialysed at 4 °C for 24 h against PBS 1x (136 mM NaCl, 2.7 mM KCl, 3.2 mM Na_2HPO_4, 1.5 mM KH_2PO_4, pH 7.5) supplemented with Arg and Glu at 50 mM in order to favour the stability of the proteins (Golovanov et al., 2004). The purified recombinant proteins were analyzed and quantified by SDS-15% PAGE after Coomassie brilliant blue staining.

EMSA

A ^{32}P-labeled ssRNA probe named 5′-PFBV and embracing the 5′-terminal 141 nt of PFBV genome was used for EMSA. The ^{32}P-labeled RNA probe (at 97 pM) was mixed with p12 and derivatives at different ratios in 25 μl of binding buffer (50 mM Tris-HCl, pH 8.0, 50 mM NaCl, 0.1 mM EDTA, 10% glycerol and 2 U of RNase inhibitor [Fermentas]) and incubated at 25 °C for 30 min. When indicated, the NaCl concentration was modified. After the binding reaction, samples were analyzed by non-denaturing PAGE (5%) in TAE buffer (40 mM Tris-HCl, 20 mM sodium acetate, 1 mM EDTA, pH 7.2). The gel was vacuum dried and exposed for autoradiography or phosphorimage analysis. In competition experiments, different amounts of unlabeled nucleic acids were added simultaneously with the labeled ssRNA probe to the binding mixtures. Competitors corresponded to two distinct ssRNAs, namely 3′-PFBV (encompassing nt 3560–3923 of the PFBV genome) and het-ssRNA (non-PFBV ssRNA), and to heterologous dsRNA, ssDNA and dsDNA molecules. Synthesis of the labelled probe and of the different competitors was performed as previously described (Martínez-Turiño and Hernández, 2010). GraphPad Prism software version 5.03 was employed for non-linear regression analysis of the binding data and for estimation of K_d and IC_{50} values.

Northwestern assay

Recombinant proteins pET-p12(1–59), pET-p12(26–106), pET-p12(1–59)m2R, pET-p12(1–59)m3R and pET-p12(1–59)m4R were electrophoresed through 15% SDS-polyacrylamide gels and electroblotted to nitrocellulose membranes (Scheicher and Schuell) in the presence of transfer buffer (25 mM Tris, 192 mM glycine and 20% methanol). The membrane attached proteins were renatured overnight at room temperature in renaturation buffer (10 mM Tris– HCl pH 7.5, 1 mM EDTA, 50 mM NaCl, 0.1% Triton X-100 and 1× Denhardt's reagent) supplemented with 1% BSA. The membranes were then probed with ^{32}P- labelled 3′-PFBV ssRNA, washed three times with the renaturation buffer, air dried and subjected to autoradiography.

Sequence analyses

A consensus secondary structure of PFBV p12 was drawn from data obtained by means of SYMPRED server (http://www.ibi.vu.nl/programs/sympredwww/) (Simossis and Heringa, 2004), that was run using a combination of different programs (JNet, PSIPred PHDpsi, SSPro2.01, YASPIN and PREDATOR). Hydrophobic regions with potential membrane insertion were determined through programs SOUSI, TMPRED, DAS, TMHMM2 HMMTop 2.0 and TopPred2 available at the Expasy Proteomics server (http://expasy.org/tools/#proteome) (Gasteiger et al., 2003). Softwares NetPhos 2.0 and YinOYang 1.2 were used from the same server for prediction of potential phosphorylation and glycosylation sites in the protein.

Acknowledgments

We gratefully thank Dr. Vicente Pallás for critical reading of the manuscript and Dolores Arocas and Isabella Avellaneda for their technical assistance. This research was supported by grant BFU2006-11230 and BFU2009-11699 from the Ministerio Ciencia e Innovación (MICINN, Spain) and by grants ACOM/2006/210 and ACOMP/2009/040 (Generalitat Valenciana, GV) to C. H. S. M.-T. was the recipient of a predoctoral fellowship from GV and of a predoctoral contract from MICINN.

References

Akgoz, M., Nguyen, Q.N., Talmadge, A.E., Drainville, K.E., Wobbe, K.K., 2001. Mutational analysis of *Turnip crinkle virus* movement protein p8. Mol. Plant Pathol. 2, 37–48.
Ansel-McKinney, P., Scott, S.W., Swanson, M., Ge, X., Gehrke, L., 1996. A plant viral coat protein RNA binding consensus sequence contains a crucial arginine. EMBO J. 15, 5077–5084.
Benitez-Alfonso, Y., Faulkner, C., Ritzenthaler, C., Maule, A., 2010. Plasmodesmata: gateways to local and systemic virus infection. Mol. Plant-Microbe Interact. 23, 1403–1412.
Bornberg-Bauer, E., Rivals, E., Vingron, M., 1998. Computational approaches to identify leucine zippers. Nucleic Acids Res. 26, 2740–2746.
Brantley, J.D., Hunt, A.G., 1993. The N-terminal protein of the polyprotein encoded by the potyvirus *Tobacco vein mottling virus* is an RNA-binding protein. J. Gen. Virol. 74, 1157–1162.
Brill, L.M., Nunn, R.S., Kahn, T.W., Yeager, M., Beachy, R.N., 2000. Recombinant *Tobacco mosaic virus* movement protein is an RNA-binding, alpha-helical membrane protein. Proc. Natl. Acad. Sci. USA 97, 7112–7117.
Busch, S.J., Sassone-Corsi, P., 1990. Dimers, leucine zippers and DNA-binding domains. Trends Genet. 6, 36–40.
Chen, Y., Varani, G., 2005. Protein families and RNA recognition. FEBS J. 272, 2088–2097.
Chevalier, F., Perazza, D., Laporte, F., Le Hénanff, G., Hornitschek, P., Bonneville, J.M., Herzog, M., Vachon, G., 2008. GeBP and GeBP-like proteins are noncanonical leucine-zipper transcription factors that regulate cytokinin response in *Arabidopsis*. Plant Physiol. 146, 1142–1154.
Citovsky, V., Knorr, D., Schuster, G., Zambryski, P., 1990. The P30 movement protein of *Tobacco mosaic virus* is a single strand nucleic acid binding protein. Cell 60, 637–647.
Daròs, J.A., Carrington, J.C., 1997. RNA binding activity of NIa proteinase of *Tobacco etch potyvirus*. Virology 237, 327–336.
Desvoyes, B., Faure-Rabasse, S., Chen, M.H., Park, J.W., Scholthof, H.B., 2002. A novel plant homeodomain protein interacts in a functionally relevant manner with a virus movement protein. Plant Physiol. 129, 1521–1532.
Fetchko, M., Stagljar, I., 2004. Application of the split-ubiquitin membrane yeast two-hybrid system to investigate membrane protein interactions. Methods 32, 349–362.
Fry, A.M., Arnaud, L., Nigg, E.A., 1999. Activity of the human centrosomal kinase, Nek2, depends on an unusual leucine zipper dimerization motif. J. Biol. Chem. 274, 16304–16310.
Gasteiger, E., Gattiker, A., Hoogland, C., Ivanyi, I., Appel, R.D., Bairoch, A., 2003. ExPASy: The proteomics server for in-depth protein knowledge and analysis. Nucleic Acids Res. 31, 3784–3788.
Genovés, A., Navarro, J.A., Pallás, V., 2006. Functional analysis of the five *Melon necrotic spot virus* genome-encoded proteins. J. Gen. Virol. 87, 2371–2380.
Genovés, A., Navarro, J.A., Pallás, V., 2009. A self-interacting carmovirus movement protein plays a role in binding of viral RNA during the cell-to-cell movement and shows an actin cytoskeleton dependent location in cell periphery. Virology 395, 133–142.
Genovés, A., Navarro, J.A., Pallás, V., 2010. The intra- and intercellular movement of *Melon necrotic spot virus* (MNSV) depends on an active secretory pathway. Mol. Plant-Microbe Interact. 23, 263–272.
Golovanov, A.P., Hautbergue, G.M., Wilson, S.A., Lian, L.Y., 2004. A simple method for improving protein solubility and long-term stability. J. Am. Chem. Soc. 126, 8933–8939.
Hacker, D.L., Petty, I.T., Wei, N., Morris, T.J., 1992. *Turnip crinkle virus* genes required for RNA replication and virus movement. Virology 186, 1–8.
Hans, F., Fuchs, M., Pinck, L., 1992. Replication of *Grapevine fanleaf virus* satellite RNA transcripts in *Chenopodium quinoa* protoplasts. J. Gen. Virol. 73, 2517–2523.
Harries, P.A., Schoelz, J.E., Nelson, R.S., 2010. Intracellular transport of viruses and their components: utilizing the cytoskeleton and membrane highways. Mol. Plant-Microbe Interact. 23, 1381–1393.
Haupt, S., Cowan, G.H., Ziegler, A., Roberts, A.G., Oparka, K.J., Torrance, L., 2005. Two plant-viral movement proteins traffic in the endocytic recycling pathway. Plant Cell 17, 164–181.
Heinlein, M., Epel, B.L., 2004. Macromolecular transport and signaling through plasmodesmata. Int. Rev. Cytol. 235, 93–164.
Heinlein, M., Padgett, H.S., Gens, J.S., Pickard, B.G., Casper, S.J., Epel, B.L., Beachy, R.N., 1998. Changing patterns of localization of the *Tobacco mosaic virus* movement protein and replicase to the endoplasmic reticulum and microtubules during infection. Plant Cell 10, 1107–1120.
Herranz, M.C., Pallás, V., 2004. RNA-binding properties and mapping of the RNA-binding domain from the movement protein of *Prunus necrotic ringspot virus*. J. Gen. Virol. 85, 761–768.
Hull, R., 2002. Virus movement through the plant and effects on plant metabolism, Matthews' plant virology, 4th Ed. Academic Press, San Diego, pp. 373–436.
Ju, H.J., Samuels, T.D., Wang, Y.S., Blancaflor, E., Payton, M., Mitra, R., Krishnamurthy, K., Nelson, R.S., Verchot-Lubicz, J., 2005. The *Potato virus X* TGBp2 movement protein associates with endoplasmic reticulum-derived vesicles during virus infection. Plant Physiol. 138, 1877–1895.
Kawakami, S., Hori, K., Hosokawa, D., Okada, Y., Watanabe, Y., 2003. Defective tobamovirus movement protein lacking wild-type phosphorylation sites can be complemented by substitutions found in revertants. J. Virol. 77, 1452–1461.

Knoester, M., van Loon, L.C., van den Heuvel, J., Hennig, J., Bol, J.F., Linthorst, H.J.M., 1998. Ethylene-insensitive tobacco lacks nonhost resistance against soil-borne fungi. Proc. Natl. Acad. Sci. USA 95, 1933–1937.

Landschulz, W.H., Johnson, P.F., McKnight, S.L., 1998. The leucine zipper: a hypothetical structure common to a new class of DNA binding proteins. Science 240, 1759–1764.

Leh, V., Jacquot, E., Geldreich, A., Haas, M., Blanc, S., Keller, M., Yot, P., 2001. Interaction between the open reading frame III product and the coat protein is required for transmission of *Cauliflower mosaic virus* by aphids. J. Virol. 75, 100–106.

Li, W.Z., Qu, F., Morris, T.J., 1998. Cell-to-cell movement of *Turnip crinkle virus* is controlled by two small open reading frames that function *in trans*. Virology 244, 405–416.

Liang, X.Z., Lee, B.T.K., Wong, S.M., 2002a. Covariation in the capsid protein of *Hibiscus chlorotic ringspot virus* induced by serial passaging in a host that restricts movement leads to avirulence in its systemic host. J. Virol. 76, 12320–12324.

Liang, X.Z., Lucy, A.P., Ding, S.W., Wong, S.M., 2002b. The p23 protein of *Hibiscus chloritc ringspot virus* is indispensable for host-specific replication. J. Virol. 76, 12312–12319.

Lommel, S.A., Martelli, G.P., Rubino, L., Russo, M., 2005. Family *Tombusviridae*. In: Fauquet, C.M., Mayo, M.A., Maniloff, J., Desselberger, U., Ball, L.A. (Eds.), Eighth Report of the International Committee on Taxonomy of Viruses. Academic Press, San Diego, USA, pp. 907–936.

Long, G., Pan, X., Vlak, J.M., 2008. Conserved leucines in N-terminal heptad repeat HR1 of envelope fusion protein F of group II nucleopolyhedroviruses are important for correct processing and essential for fusogenicity. J. Virol. 82, 2437–2447.

López, C., Navas-Castillo, J., Gowda, S., Moreno, P., Flores, R., 2000. The 23-kDa protein coded by the 3′-terminal gene of *Citrus tristeza virus* is an RNA-binding protein. Virology 269, 462–470.

Luan, C.H., Qiu, S., Finley, J.B., Carson, M., Gray, R.J., Huang, W., Johnson, D., Tsao, J., Reboul, J., Vaglio, P., Hill, D.E., Vidal, M., Delucas, L.J., Luo, M., 2004. High-throughput expression of *C. elegans* proteins. Genome Res. 14, 2102–2110.

Lucas, W.J., 2006. Plant viral movement proteins: agents for cell-to-cell trafficking of viral genomes. Virology 344, 169–184.

Lyu, P.C., Liff, M.I., Marky, L.A., Kallenbach, N.R., 1990. Side chain contributions to the stability of alpha-helical structure in peptides. Science 250, 669–673.

Marcos, J.F., Vilar, M., Pérez-Payá, E., Pallás, V., 1999. *In vivo* detection, RNA-binding properties and characterization of the RNA-binding domain of the p7 putative movement protein from carnation mottle carmovirus (CarMV). Virology 255, 354–365.

Martínez-Gil, L., Johnson, A.E., Mingarro, I., 2010. Membrane insertion and biogenesis of the *Turnip crinkle virus* p9 movement protein. J. Virol. 84, 5520–5527.

Martínez-Turiño, S., Hernández, C., 2009. Inhibition of RNA silencing by the coat protein of *Pelargonium flower break virus*: distinctions from closely related suppressors. J. Gen. Virol. 90, 519–525.

Martínez-Turiño, S., Hernández, C., 2010. Identification and characterization of RNA binding activity in the ORF1-encoded replicase protein of *Pelargonium flower break virus*. J. Gen. Virol. 91, 3075–3084.

Melcher, U., 2000. The '30K' superfamily of viral movement proteins. J. Gen. Virol. 81, 257–266.

Moitra, J., Szilák, L., Krylov, D., Vinson, C., 1997. Leucine is the most stabilizing aliphatic amino acid in the d position of a dimeric leucine zipper coiled coil. Biochemistry 36, 12567–12573.

Navarro, J.A., Genovés, A., Climent, J., Saurí, A., Martínez-Gil, L., Mingarro, I., Pallás, V., 2006. RNA-binding properties and membrane insertion of *Melon necrotic spot virus* (MNSV) double gene block movement proteins. Virology 356, 57–67.

Nelson, R.S., Citovsky, V., 2005. Plant viruses. Invaders of cells and pirates of cellular pathways. Plant Physiol. 138, 1809–1814.

O'Neil, K.T., DeGrado, W.F., 1990. A thermodynamic scale for the helix-forming tendencies of the commonly occurring amino acids. Science 250, 646–651.

O'Shea, E.K., Rutkowski, R., Kim, P.S., 1989. Evidence that the leucine zipper is a coiled coil. Science 243, 538–542.

Pagano, M., Clynes, M.A., Masada, N., Ciruela, A., Ayling, L.J., Wachten, S., Cooper, D.M., 2009. Insights into the residence in lipid rafts of adenylyl cyclase AC8 and its regulation by capacitative calcium entry. Am. J. Physiol. Cell Physiol. 296, C607–C619.

Peremyslov, V.V., Pan, Y.W., Dolja, V.V., 2004. Movement protein of a closterovirus is a type III integral transmembrane protein localized to the endoplasmic reticulum. J. Virol. 78, 3704–3709.

Rao, A.L., Grantham, G.L., 1996. Molecular studies on bromovirus capsid protein. II. Functional analysis of the amino-terminal arginine-rich motif and its role in encapsidation, movement, and pathology. Virology 226, 294–305.

Richmond, K.E., Chenault, K., Sherwood, J.L., German, T.L., 1998. Characterization of the nucleic acid binding properties of *Tomato spotted wilt virus* nucleocapsid protein. Virology 248, 6–11.

Rico, P., Hernández, C., 2004. Complete nucleotide sequence and genome organization of *Pelargonium flower break virus*. Arch. Virol. 149, 641–651.

Rico, P., Hernández, C., 2006. Infectivity of *in vitro* transcripts from a full length cDNA clone of *Pelargonium flower break virus* in an experimental and a natural host. J. Plant Pathol. 88, 103–106.

Rico, P., Hernández, C., 2009. Characterization of the subgenomic RNAs produced by *Pelargonium flower break virus*: identification of two novel RNA species. Virus Res. 142, 100–107.

Rico, P., Ivars, P., Elena, S.F., Hernández, C., 2006. Insights on the selective pressures restricting *Pelargonium flower break virus* genome variability: evidence for host adaptation. J. Virol. 80, 8124–8132.

Ruiz, M.T., Voinnet, O., Baulcombe, D.C., 1998. Initiation and maintenance of virus-induced gene silencing. Plant Cell 10, 937–946.

Sambrook, J., Fritsch, E.F., Maniatis, T., 2007. Molecular Cloning: A Laboratory Manual. Cold Spring Harbor Laboratory Press, Cold Spring Harbor, N.Y., U.S.A.

Saurí, A., Saksena, S., Salgado, J., Johnson, A.E., Mingarro, I., 2005. Double-spanning plant viral movement protein integration into the endoplasmic reticulum membrane is signal recognition particle-dependent, translocon-mediated, and concerted. J. Biol. Chem. 280, 25907–25912.

Schepetilnikov, M.V., Solovyev, A.G., Gorshkova, E.N., Schiemann, J., Prokhnevsky, A.I., Dolja, V.V., Morozov, S.Y., 2008. Intracellular targeting of a hordeiviral membrane-spanning movement protein: sequence requirements and involvement of an unconventional mechanism. J. Virol. 82, 1284–1293.

Simossis, V.A., Heringa, J., 2004. Optimally segmented consensus secondary structure predictionSYMPRED server at URL: http://ibivu.cs.vu.nl/programs/sympredwww/2004.

Skuzeski, J.M., Morris, T.J., 1995. Quantitative analysis of the binding of *Turnip crinkle virus* coat protein to RNA fails to demonstrate binding specificity but reveals a highly cooperative assembly interaction. Virology 210, 82–90.

Takemoto, Y., Hibi, T., 2005. Self-interaction of ORF II protein through the leucine zipper is essential for *Soybean chlorotic mottle virus* infectivity. Virology 332, 199–205.

Takemoto, Y., Kanehira, T., Shinohara, M., Yamashita, S., Hibi, T., 2000. The nucleotide sequence and genome organization of *Japanese iris necrotic ring virus*, a new species in the genus *Carmovirus*. Arch. Virol. 145, 651–657.

Verwoerd, T.C., Dekker, B.M.M., Hoekema, A., 1989. A small-scale procedure for the rapid isolation of plant RNAs. Nucleic Acids Res. 17, 2362.

Vilar, M., Esteve, V., Pallás, V., Marcos, J.F., Pérez-Payá, E., 2001. Structural properties of *Carnation mottle virus* p7 movement protein and its RNA-binding domain. J. Biol. Chem. 276, 18122–18129.

Vilar, M., Saurí, A., Monné, M., Marcos, J.F., von Heijne, G., Pérez-Payá, E., Mingarro, I., 2002. Insertion and topology of a plant viral movement protein in the endoplasmic reticulum membrane. J. Biol. Chem. 277, 23447–23452.

Vilar, M., Saurí, A., Marcos, J.F., Mingarro, I., Pérez-Payá, E., 2005. Transient structural ordering of the RNA-binding domain of *Carnation mottle virus* p7 movement protein modulates nucleic acid binding. Chembiochem 6, 1391–1396.

Waigmann, E., Ueki, S., Trutnyeva, K., Citovsky, V., 2004. The ins and outs of non-destructive cell-to-cell and systemic movement of plant viruses. Crit. Rev. Plant Sci. 23, 195–250.

Weiss, M.A., Narayana, N., 1998. RNA recognition by arginine-rich peptide motifs. Biopolymers 48, 167–180.

Wobbe, K.K., Akgoz, M., Dempsey, D.A., Klessig, D.F., 1998. A single amino acid change in *Turnip crinkle virus* movement protein p8 affects RNA binding and virulence on *Arabidopsis thaliana*. J. Virol. 72, 6247–6250.

Zhang, X.J., Baase, W.A., Matthews, B.W., 1991. Toward a simplification of the protein folding problem: a stabilizing polyalanine alpha-helix engineered in T4 lysozyme. Biochemistry 30, 2012–2017.